The invariable boundary conditions are:

$$\widehat{f}_n(0) = \widehat{f}'_n(0) = \widehat{\theta}_n(0) = \widehat{\phi}_n(0) = 0, \qquad \widehat{f}''_n(\beta) = \widehat{\theta}'_n(\beta) = \widehat{\phi}'_n(\beta) = 0 \quad (3.\ 52)$$

Here

$$R_n^f(\eta) = (1+k)\widehat{f}'''_{n-1} - \sum_{k=0}^{n-1} \widehat{f}'_{n-1-k}\widehat{f}'_k + \sum_{k=0}^{n-1} \widehat{f}_{n-1-k}\widehat{f}''_k - A\left[\widehat{f}'_{n-1} + \frac{\eta}{2}\widehat{f}''_{n-1}\right] + \lambda \sum_{k=0}^{n-1} \left(\widehat{f}''_{n-1-k}\right)^2 \widehat{f}'''_k - M\widehat{f}'_{n-1} - k^*\widehat{f}'_{n-1}. \quad (3.\ 53)$$

$$R_n^\theta(\eta) = \left(1+\xi\theta\right)\widehat{\theta}''_{n-1} + \frac{1}{Pr}\xi \sum_{k=0}^{n-1} \widehat{\theta}_{n-1-k}\widehat{\theta}''_k + \sum_{k=0}^{n-1} \widehat{f}_{n-1-k}\widehat{\theta}'_k - 2\sum_{k=0}^{n-1} \widehat{f}'_{n-1-k}\widehat{\theta}_k - \frac{A}{2}\left(3\widehat{\theta}_{n-1} + \eta\widehat{\theta}'_{n-1}\right) + Nb\sum_{k=1}^{n-1} \widehat{\theta}'_{n-1-k}\widehat{\phi}'_k + Nt\sum_{k=1}^{n-1} \widehat{\theta}'_{n-1-k}\widehat{\theta}'_k. \quad (3.\ 54)$$

$$R_n^\phi(\eta) = \widehat{\phi}''_{n-1} + Sc\sum_{k=0}^{n-1} \widehat{f}_{n-1-k}\widehat{\phi}'_k - 2Sc\sum_{k=0}^{n-1} \widehat{f}'_{n-1-k}\widehat{\phi}_k - \frac{ASc}{2}\left(3\widehat{\phi}_{n-1} + \eta\widehat{\phi}'_{n-1}\right) + \frac{Nt}{Nb}\widehat{\theta}''_{n-1} \quad (3.\ 55)$$

Where

$$\chi_n = \begin{cases} 1, & \zeta > 1 \\ 0, & \zeta \leqslant 1 \end{cases} \quad (3.\ 56)$$

4. CONVERGENCE:

When we computed the series solutions of velocity, temperature and concentration functions using HAM, the assisting parameters $h_{f,\theta}$ and h_ϕ appears, which are responsible for adjusting the convergence of solutions. h-curve graphs of $f''(0)$,$\theta'(0)$ and $\phi'(0)$ for 7^{th} order Approximation are plotted to get the possible region of h curve in the Figures (2-3) for various values of embedded variables. The h-curves consecutively display the valid region. The convergence region of the h-curve in Figs. 2 and 3 is shown as $-0.2 \leq h \leq 0.0$ which is a valid region.

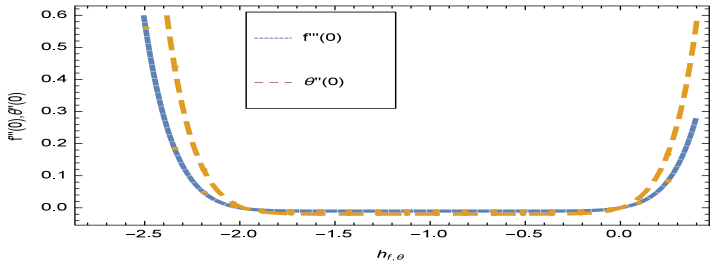

FIGURE 2. Combine h curve of function f and θ at 7^{th} order approximation, when $\gamma = Sc = A = \xi = \beta = k = 0.1$, $Nb = Nt = 0.3$, $M = Pr = 1$.

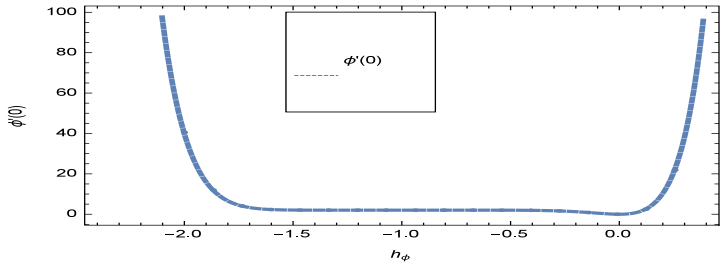

FIGURE 3. The h curve function of ϕ for 7^{th} order approximation, when $\gamma = Sc = A = \xi = \beta = k = 0.1$, $Nb = Nt = 0.3$, $M = Pr = 1$.

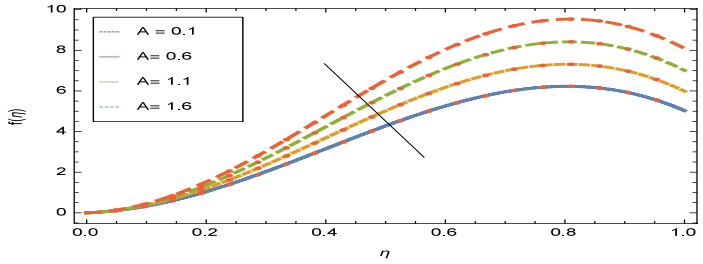

FIGURE 4. Influence of A on $f(\eta)$, where $\beta = 0.4$,$M = 1$,$\gamma = 0.7$,$\lambda = k = 0.6$.

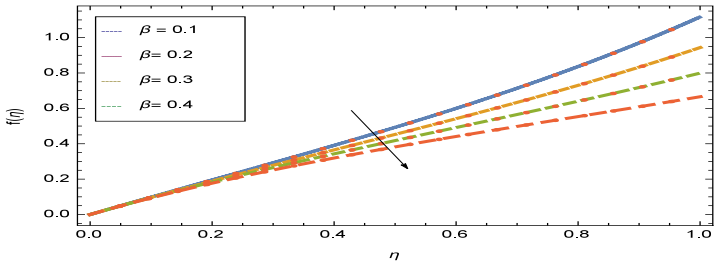

FIGURE 5. Influence of β on $f(\eta)$, where $A = 0.1, M = 1, \gamma = 0.7, \lambda = k = 0.6$.

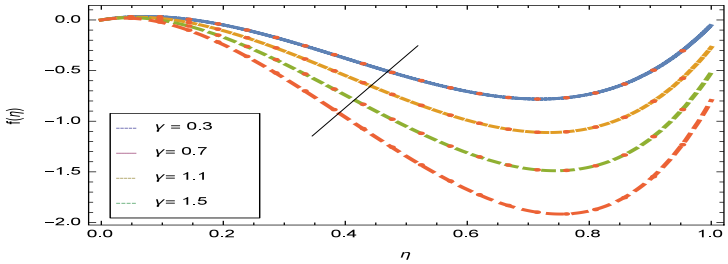

FIGURE 6. Influence of γ on $f(\eta)$, where $\beta = 0.4, M = 1, A = 0.9, \lambda = 0.5, k = 0.6$.

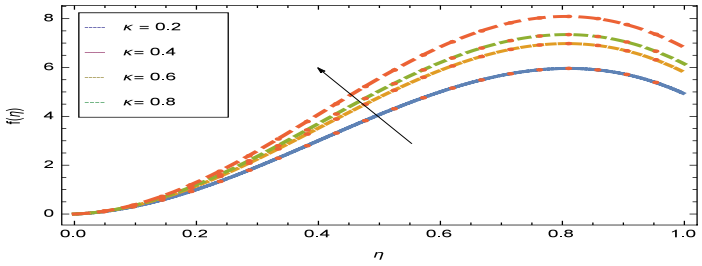

FIGURE 7. Influence of k on $f(\eta)$, where $\beta = 0.4, M = 1, A = 0.9, \lambda = \gamma = 0.5$.

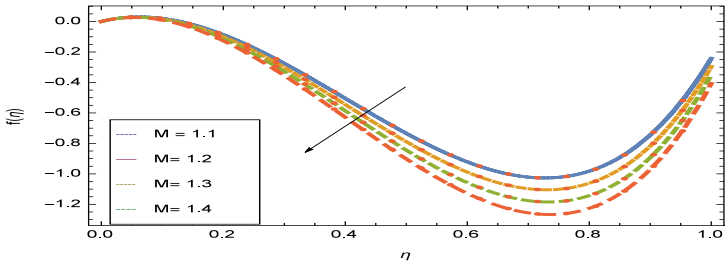

FIGURE 8. Influence of M on $f(\eta)$, where $\beta = 0.4$,$\gamma = 0.7$,$\lambda = 0.3$,$A = 0.9$,$k = 0.6$.

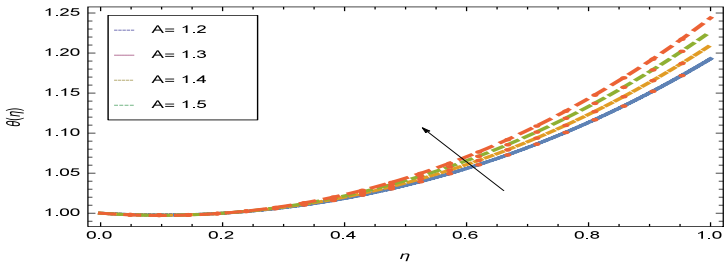

FIGURE 9. Influence of A on $\theta(\eta)$, where $\gamma = Sc = \xi = 0.6$, $\beta = 0.1$,$Nb = 0.3$, $M = 0.5$, $Nt = k = 0.4$, $Pr = 1$.

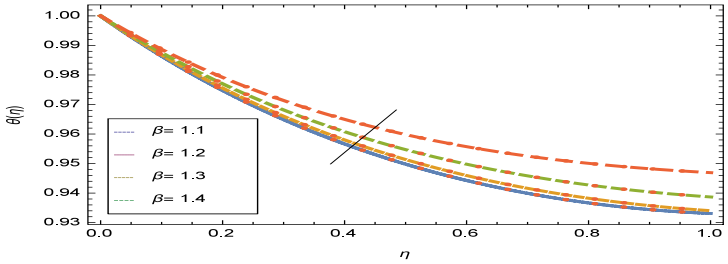

FIGURE 10. Influence of β on $\theta(\eta)$, where $\gamma = A = Sc = \xi = 0.6$,$M = 0.1$,$Nb = 0.3$, $Nt = k = 0.4$,$Pr = 1$.

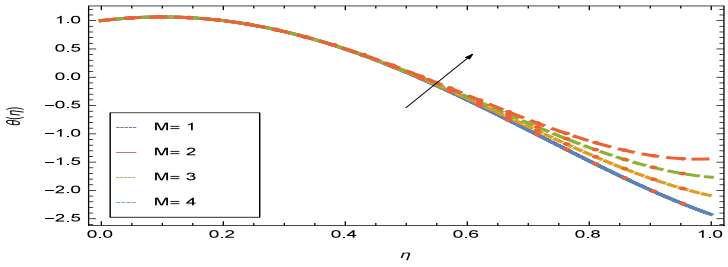

FIGURE 11. Influence of M on $\theta(\eta)$, where $\gamma = A = Sc = \xi = 0.6$,$\beta = 0.1$,$Nb = 0.3$, $Nt = k = 0.4$,$Pr = 1$.

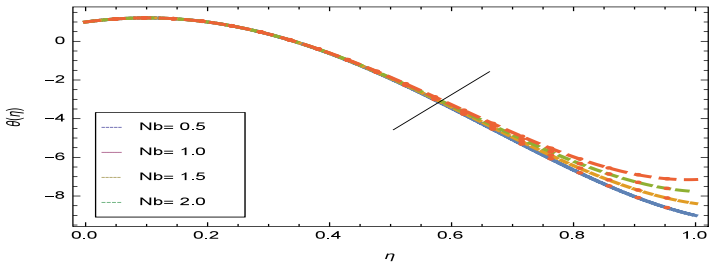

FIGURE 12. Influence of Nb on $\theta(\eta)$, where $\gamma = A = Sc = \xi = 0.6$,$\beta = 0.1$,$M = 0.5$,$Nt = Rd = k = 0.4$,$Pr = 1$.

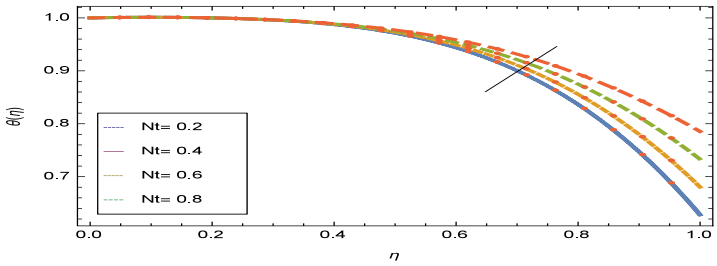

FIGURE 13. Influence of Nt on $\theta(\eta)$, where $\gamma = A = Sc = \xi = 0.6$,$\beta = 0.1$,$M = 0.5$,$Nb = 0.3$,$Rd = k = 0.4$,$Pr = 1$.

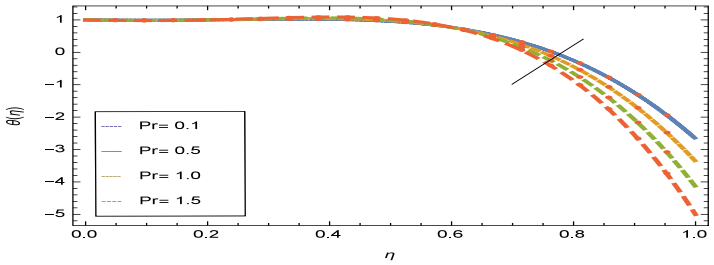

FIGURE 14. Influence of Pr on $\theta(\eta)$, where $\gamma = A = Sc = \xi = 0.6$,$\beta = 0.1$,$M = 5$,$Nb = 3$, $Nt = Rd = k = 0.4$.

FIGURE 15. Influence of Sc on $\theta(\eta)$, where $\gamma = A = \xi = 0.6$,$\beta = 0.1$,$M = 0.2$,$Nb = 0.3$, $Nt = k = 0.4$, $Pr = 1$.

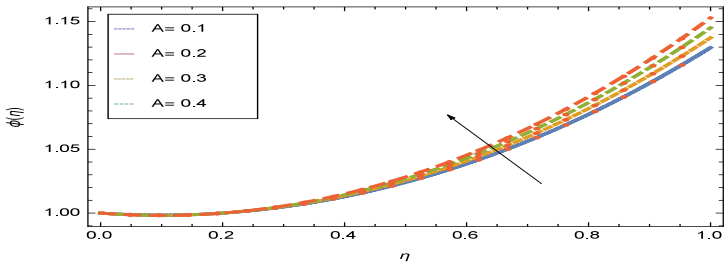

FIGURE 16. Influence of A on $\phi(\eta)$, where $\gamma = Sc = \xi = 0.6$,$\beta = 0.1$,$M = 0.5$,$Nb = 0.3$, $Nt = k = 0.4$, $Pr = 1$.

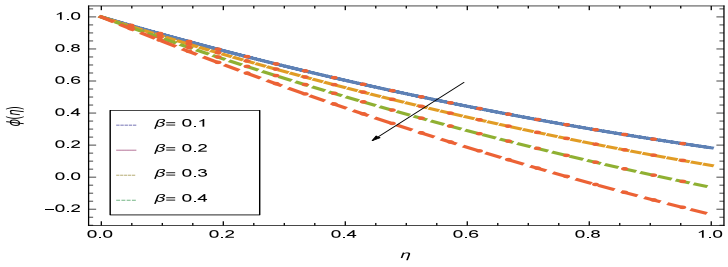

FIGURE 17. Influence of β on $\phi(\eta)$, where $\gamma = 1.9$,$Sc = 0.3$,$\xi = 1.1$,$M = 0.2$, $Nb = 0.5$, $A = 1.2$, $Nt = 0.5$, $k = Pr = 0.1$.

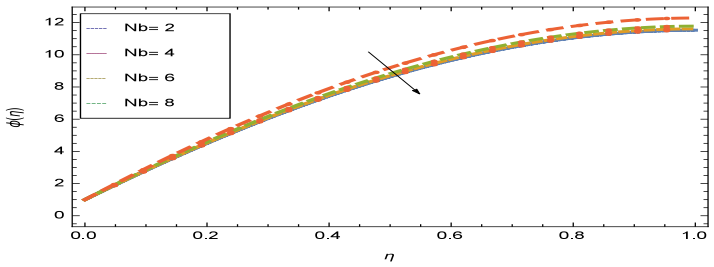

FIGURE 18. Influence of Nb on $\phi(\eta)$, where $\gamma = Sc = \xi = 0.6$,$\beta = 1$,$M = 0.1$,$A = 0.5$, $Nt = k = 0.4$, $Pr = 1$.

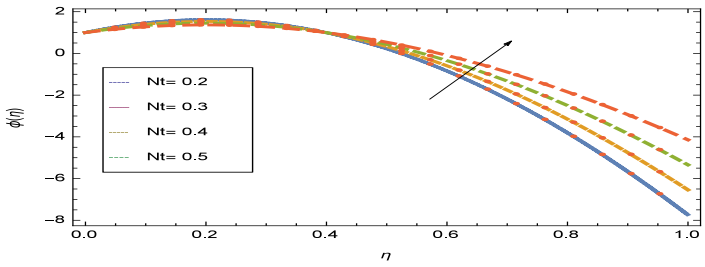

FIGURE 19. Influence of Nt on $\phi(\eta)$, where $\gamma = Sc = \xi = 0.6$, $\beta = 0.2$,$M = 0.1$, $Nb = A = 0.5$, $k = 0.5$, $Pr = 1$.

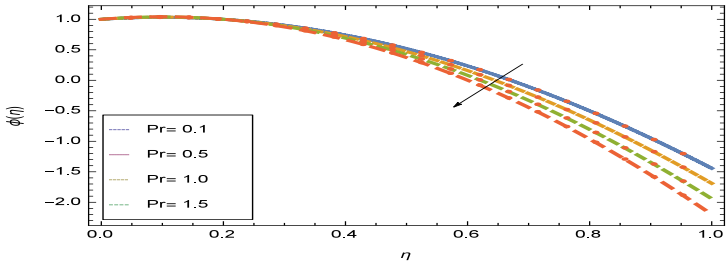

FIGURE 20. Influence of Pr on $\phi(\eta)$, where $\gamma = Sc = A = \xi = 0.6$,$\beta = 0.1$,$M = Nb = Nt = 0.5$, $k = 0.4$.

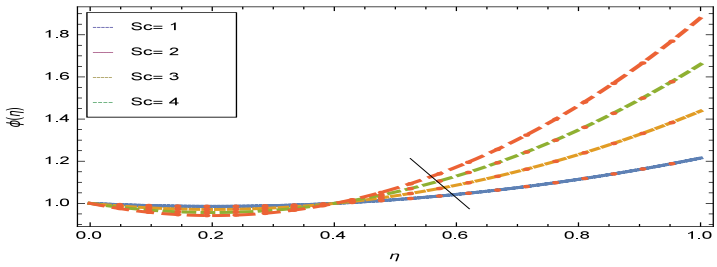

FIGURE 21. Influence of Sc on $\phi(\eta)$, where $\gamma = \xi = 0.6$, $\beta = 0.2$, $M = 0.1$,$Nb = A = 0.5$, $Nt = k = 0.4$, $Pr = 1$.

5. TABLES DISCUSSION

This section is about the discussion of tables. Table.1 displays numerical values of HAM solutions at different approximation using different values for various parameters. Clearly the table values shows that homotopy analysis technique is a quickly convergent technique. Table quantities such as film thickness β, skin friction co-efficient $f''(0)$, heat flux $Nu = -\theta'(0)$ and mass flux $Sh = -\phi'(0)$ for engineering interest are calculated from Tables 2,3 and 4. In Table.2 values of skin friction co-efficient $f''(0)$ and thin film thickness β are determined using increasing values of A. It is analyzed that skin friction co-efficient increases and the thin film thickness reduces randomly with increasing values of A. In table.3 the effect of M, Nt, A and Pr on wall temperature is calculated taking $A = 0.8$ the large value of M and Nt increase the wall temperature while the large value of A and Pr reduces the wall temperature. Table.4 examines the effect of embedding parameters Nb, β, Pr and Nt on the heat flux $Nu = -\theta'(0)$ and mass flux $Sh = -\phi'(0)$. It has been seen that the increasing values of Nb, β and Pr decreases mass flux while the increasing values of Nt increases mass flux. It has also been seen that the increasing values of embedded parameters randomly varies heat flux. The current results of $-\theta'(0)$ and $-\phi'(0)$ having a resemblance in appearance.

Table 1. Convergence of $f''(0)$, $\theta'(0)$ and $\phi'(0)$ by HAM Method when $Nt = Nb = 0.3$, $A = Sc = k = \xi = \gamma = \beta = 0.1$, $Pr = M = 1$.

Solution Approximation	$f''(0)$	$\theta'(0)$	$\phi'(0)$
1	-0.05401	-0.10070	-1.10075
4	-0.10218	-0.18890	-1.38506
7	-0.10813	-0.19903	-1.88867
10	-0.10888	-0.20281	-1.99293
13	-0.10894	-0.20154	-2.01113
14	-0.10896	-0.20475	-2.01406
17	-0.10897	-0.20478	-2.01451
20	-0.10897	-0.20479	-2.01458
25	-0.10897	-0.20479	-2.01458

Table 2. Results of skin friction coefficient $f''(0)$ and film thickness β for various values of A.

A	Present Results $f''(0)$	Present Results β
0.4	-4.33027	5.523451
0.6	-3.94882	4.002111
0.8	-2.64208	3.992358
1.0	-1.33999	3.113001
1.2	-0.92157	1.625391
1.4	-0.56897	1.896541
1.6	-0.34227	0.876512
1.8	-0.03027	0.266156

Table 3. The wall temperature for dissimilar values of M, A, Pr and Nt when $A = 0.8$,$Nb = 0.4$,$\beta = 0.9$,$Nb = 1.6$

M	Nt	A	Pr	Present (2017) Results $\theta(\beta)$
0	0.1	1.0	0.1	0.223456
1				0.432111
2	0.01			0.712351
	0.1	0.0		1.023001
		1.0	0.1	1.625341
			0.2	1.236540

Table 4. The Nusslet number $\phi'(0)$ and Sherwood numbers $\theta'(0)$ verses various value of embedded parameters when $A = 0.8$.

Nb	β	Pr	Nt	$-\theta'(0)$ Present Results	$-\phi'(0)$ Present Results
0.0	0.2	1.0	0.1	0.682385	6.68238
0.5				0.541422	4.94142
1.0				0.440569	5.44569
	0.2			0.321022	5.12101
	0.3			0.300420	5.70742
	0.4			0.291420	5.29140
		0.5		0.371420	5.37143
		1.5		0.182285	6.78223
		5.0		0.011422	7.01147
			0.4	0.612427	4.11207
			0.6	0.691428	4.69458
			0.8	0.500987	7.50097

6. DISCUSSION:

The present work focuses on the comprehension of the fluid film motion through modeled parameters.The graphical explanation of these parameters have been illustrated in figures [4-21] while Fig.2 is the combine h curve graph of velocity and temperature profiles and Fig.3 is the h curve graph of concentration profile.Both the graphs reflect valid region which gaurantees that homotopy analysis method is fast convergent technique.The influence of unsteady constraint A on the $\widehat{f}(\eta)$ field shown in Fig.4.The velocity profile $\widehat{f}(\eta)$ rises with the rise in A. Velocity increases with the unsteady constraint A.The influance of film thickness β has been displayed for unlike values of fluid velocity in Fig.5.It is observed that $\widehat{f}(\eta)$ falls over with greater values of β.The impact of stretching parameter γ on the $\widehat{f}(\eta)$ has been shown in Fig.6. It has been seen that $\widehat{f}(\eta)$ decreases with the

growing values of stretching parameter.The effect of Erying fluid factor k over the $\widehat{f}(\eta)$ is exposed in Fig.7.It has been seen, when Erying fluid parameter k increases then it increases the nanofluid film motion, and this influance is clear at the stretching surface.The characteristics of magnetic factor M on fluid velocity and heat profile are shown in Figs.8 and 11.It is obvious from mathematical formulation that M is inversely varied with velocity flied $\widehat{f}(\eta)$.Increasing M decreases the velocity field.This effect of magnetic field is caused by the production of friction force to the movement known as Lorentz force which bring retardation to the flow of the fluid and hence decreases fluid velocity at the upper surface.It is clear from Fig.16 that all the fluids reflect the similar reaction to the unsteady parameter.The slope in the temperature distribution falls down with decreasing the width of thermal boundary layers.It means that unsteady parameter A has inverse effect on the temperature field. Fig.9. shows that heat profile decreases with the parameter A.Every fluid observes the same effect on temperature profile for parameter A.Actually, the fluid produces resistance to the flow of film and shows a tendency to decay the velocity of fluid flow having greater values of β and it is obvious in Fig.11. The fluid film size absorbs heat that causes falls down in heat distribution.The free surface temperature is increased with the Brownian motion constraint as illustrated in Fig.12.The reality is that the random movement of molecules of fluid produces collisions among the molecules.Increase in the value of Brownian motion parameter Nb, results increase in temperature of the fluid, consequently, it causes reduction in free surface nanoparticle volume fraction and is shown in Fig.18.The thermophoresis parameter Nt decreases as the temperature profile increases and it can be seen in Fig.13.The thermophoresis constraint is responsible for raise in surface temperature.The random motion of nano particles of fluid produces Brownian motion.This irregular motion of nano suspended particles is responsible for kinetic energy and it causes rise in temperature.Consequently, thermophoretic force is produced.This force produces intensity in the fluid to move away from the surface of the stretching sheet.Subsequently, the temperature inside the boundary layer rises as Nt increases.Physically, the Prandtl number is the ratio of kinematic viscidness to thermal diffusivity and is a dimensionless quantity. The value of Pr is increased if the value of thermal diffusivity is less than the momentum diffusivity.Therefore, the heat transmission at the exterior increases as the values of Pr increase while mass transmission reduces as the Prandtl number increases.The influance of Pr is shown in the Fig.14.It obviously shows that $\widehat{\theta}(\eta)$ reduces with large Pr number.The logic behind is that the large value of Prandtl number reduces thermal layer of the boundary.The consequences are more prominent for minor Prandtl quantity because of relatively greater width of thermal boundary layer.The heat distribution $\widehat{\theta}(\eta)$ increases with the change in the Schmidt number and is shown in Fig.15, and the non-dimensional concentration profile reduces with dissimilar measures of parameter Sc displayed in Fig.21.It is visible that a flow part increases in the horizontal direction by rising the Schmidt number.It clearly reflects that with rise in the Schmidt number, the flow part increases in the x-direction.The logic is that the Sc parameter is the ratio of momentum to the concentration diffusivities.The growth in Sc reduces width of fluid and causes fall down in $\widehat{\theta}(\eta)$.The viscidness dissipation effect on the nanoparticle volume fraction is insignificant for higher quantities of Schmidt numbers.The concentration of the fluid $\widehat{\phi}(\eta)$ increases as values of β grows as presented by Fig.17.The logic behind is that width of fluid film exhibit direct

proportion with thermal conductivity as well as with viscosity.As thermophoresis parameter Nt increases, concentration field elevates.Just like surface temperature, thermophoresis factor also help in increasing the exterior of nanoparticle volume fraction and is illustrated in Fig.19.The increasing values of Nt decrease the surface mass transfer rate in both steady and unsteady cases, but shows high mass transfer rate on external edge in unsteady case as compared to steady one.Concentration profile shows the inverse relation with Pr number as shown in Fig.20.It means thinning of thermal boundary layer increases flow in the x-direction, which is clearly exibited in the graph.

7. Concluding Remarks:

This research work analyzes two dimensional nanofluid film flow of Eyring Powell Fluid with variable heat transmission over a porous stretching sheet in the existence of uniform magnetic flied (MHD). The observation of this work depends upon the influence of variable temperature and magnetic field on nanoliquid film flows. The influence of the skin fraction, Nusslet number and Sherwood number is shown numerically.
The key points of this work are as under:

- The increasing values of Pr increases the surface temperature, where opposite effect is found for unsteady parameter A that is the large values of A reduces the surface temperature.
- Non-dimensional velocity decline in variable viscosity and magnetic parameter.
- The temperature and concentration profile both are directly proportional with magnetic field.
- It is perceived that the large value of Magnetic parameter drops the velocity distribution of the nanofluid films.
- The larger values of Brownian motion parameter rises the profile of temperature.
- Thermal boundary layer thickness reduces with rise of Sc, Nusselt number rises with rise in Prandtl number.
- Porosity parameter decrease the motion of the liquid films.
- It is observed that the temperature profile falls with the large numbers of thermophoresis parameter Nt and increases for small values.
- Augmenting the nanoparticle concentration efficiently increases the friction feature of Eyring nanofluid.
- The increasing values of Nb reduces the mass flux, where Nt increases the mass flux. The higher values of Re reduces the mass flux, while it rises with rising values of Sc.
- The convergence of the HAM method with the variation of the physical parameters observed numerically.

8. Acknowledgement

The authors are highly grateful to Professor Dr. Gohar Ali and Professor Dr. Syed Inayat Ali Shah for his constructive comments, helpful remarks, encouragement and research advise from start to finish despite all odds.The authors are also thankful to the anonymous reviewers for their fruitful comments and to the Editor-in-Chief for his dedecation and active correspondance.

9. AUTHORCONTRIBUTIONS

Conceptualization: Mohammad Ishaq and Gohar Ali, Methodology: Zahir Shah and Mohammad Ishaq, Software: Mohammad Ishaq and Sher Muhammad, Validation: Mohammad Ishaq, Gohar Ali, Syed Inayat Ali Shah and Syed Asif Hussain, Formal Analysis: Mohammad Ishaq, Investigation: Mohammad Ishaq, Resources: Zahir Shah, WritingOriginal Draft Preparation: Mohammad Ishaq, WritingReview & Editing: Mohammad Ishaq and Sher Muhammad, Visualization: Syed Inayat Ali Shah and Syed Asif Hussain, Supervision: Gohar Ali, Syed Inayat Ali Shah.

10. COMPETING INTERESTS

Authors have declared that no competing interests exist.

REFERENCES

[1] S. Abbasbandy and A. A. Shirzadi, *New application of the homotopy analysis method: Solving the Sturm-Liouville problems*, Communications in Nonlinear Science and Numerical Simulation **16**, No. 1 (2011) 112-26.

[2] S. Abbasbandy, *The application of homotopy analysis method to nonlinear equations arising in heat transfer*, Physics Letters A. **360**, No. 1 (2006) 109-13.

[3] K. A. Abro and M. A. Solangi, *Heat Transfer in Magnetohydrodynamic Second Grade Fluid with Porous Impacts using Caputo-Fabrizoi Fractional Derivatives*, Punjab Univ. j. math. **49**, No. 2 (2017) 113-125.

[4] K. A. Abro, M. Hussain and M. M. Baig, *A Mathematical Analysis of Magnetohydrodynamic Generalized BurgerFluid for Permeable Oscillating Plate*, Punjab Univ. j. math. **50**, No. 2 (2018) 97-111.

[5] A. Ali, M. Tahir, R. Safdar, A. U. Awan, M. Imran and M. Javaid, *Magnetohydrodynamic Oscillating and Rotating Flows of Maxwell Electrically Conducting Fluids in a Porous Plane*, Punjab Univ. j. math. **50**, No. 4 (2018) 61-71.

[6] HI. Andersson, JB. Aarseth and BS. Dandapat, *Heat transfer in a liquid film on an unsteady stretching surface*, International Journal of Heat and Mass Transfer **43**, No. 1 (2000) 69-74.

[7] HI. Andersson, JB. Aarseth, N. Braud and BS. Dandapat, *Flow of a power-law fluid film on an unsteady stretching surface*, Journal of Non-Newtonian Fluid Mechanics **62**, No. 1 (1996) 1-8.

[8] A. U. Awan, M. Imran, M. Athar and M. Kamran, *Exact analytical solutions for a longitudinal flow of a fractional Maxwell fluidbetween two coaxial cylinders*, Punjab Univ. j. math. **45**, (2014) 9-23.

[9] A. U. Awan, R. Safdar, M. Imran and A. Shaukat, *Effects of Chemical Reaction on the Unsteady Flow of an IncompressibleFluid over a Vertical Oscillating Plate*, Punjab Univ. j. math. **48**, No. 2 (2016) 167-182.

[10] RC. Aziz, I. Hashim and AK. Alomari, *Thin film flow and heat transfer on an unsteady stretching sheet with internal heating*, Meccanica **46**, No. 2 (2011) 349-57.

[11] S. Bashir, M. U. Ghani Khan, A. A. Shah and A. Nasir, *Towards Computational Model of Human Brain Memory*, Punjab Univ. j. math. **46**, No. 2 (2014) 35-45.

[12] CH. Chen, *Heat transfer in a power-law fluid film over a unsteady stretching sheet*, Heat and Mass Transfer **39**, No. 8 (2003) 791-6.

[13] CH. Chen, *Effect of viscous dissipation on heat transfer in a non-Newtonian liquid film over an unsteady stretching sheet*, Journal of Non-Newtonian Fluid Mechanics **135**, No. 2 (2006) 128-35.

[14] LJ. Crane, *Flow past a stretching plate*, Zeitschrift fr angewandte Mathematik und Physik ZAMP **21**, No. 4 (1970) 645-7.

[15] BS. Dandapat and ASGupta, *Flow and heat transfer in a viscoelastic fluid over a stretching sheet*, International Journal of Non-Linear Mechanics **24**, No. 3 (1989) 215-9.

[16] M. Gul, Q. A. Chaudhry, N. Abid and S. Zahid, *Simulation of Drug Diffusion in Mammalian Cell*, Punjab Univ. j. math. Vol. **47**, No. 2 (2015) 11-18.

[17] T. Hayat, M. Awais and S. Asghar, *Radiative effects in a three-dimensional flow of MHD Eyring-Powell fluid*, Journal of the Egyptian Mathematical Society **21**, No. 3 (2013) 379-84.

[18] T. Hayat, S. Nadeem and S. Asghar, *Hydromagnetic Couette flow of an Oldroyd-B fluid in a rotating system*, International Journal of Engineering Science **42**, No. 1 (2004) 65-78.

[19] M. Ishaq, G. Ali, Z. Shah, S. Islam, S. Muhammad, *Entropy Generation on Nanofluid Thin Film Flow of EyringPowell Fluid with Thermal Radiation and MHD Effect on an Unsteady Porous Stretching Sheet*, Entropy **20**, No. 6 (2018) 412.

[20] K. Karimi and A. Bahadorimrhr, *Rational Bernstein Collocation Method for Solving the Steady Flow of a Third GradeFluid in a Porous Half Space*, Punjab Univ. j. math. **49**, No. 1 (2017) 63-73.

[21] NS. Khan, T. Gul, S. Islam, A. Khan, Z. Shah, *Brownian Motion and Thermophoresis Effects on MHD Mixed Convective Thin Film Second-Grade Nanofluid Flow with Hall Effect and Heat Transfer Past a Stretching Sheet*, Journal of Nanofluids **6**, No. 5 (2017) 812-29.

[22] H. Khan, M. Haneef, Z. Shah, S. Islam, W. Khan, S. Muhammad, *The Combined Magneto hydrodynamic and electric field effect on an unsteady Maxwell nanofluid Flow over a Stretching Surface under the Influence of Variable Heat and Thermal Radiation*, Applied Sciences **8**, No. 2 (2018) 160.

[23] SJ. Liao, *On the analytic solution of magnetohydrodynamic flows of non-Newtonian fluids over a stretching sheet*, Journal of Fluid Mechanics **488**, No. 1 (2003) 189-212.

[24] S. Liao, *On the homotopy analysis method for nonlinear problems*, Applied Mathematics and Computation **147**, No. 2 (2004) 499-513.

[25] S. Liao, *An analytic solution of unsteady boundary-layer flows caused by an impulsively stretching plate*, Communications in Nonlinear Science and Numerical Simulation **11**, No. 3 (2006) 326-39.

[26] S. Liao, *Homotopy analysis method in nonlinear differential equations*, Beijing: Higher education press, 2012 Jun 22.

[27] S. Liao, *An optimal homotopy-analysis approach for strongly nonlinear differential equations*, Communications in Nonlinear Science and Numerical Simulation **15**, No. 8 (2010) 2003-16.

[28] IC. Liu and HI. Andersson, *Heat transfer in a liquid film on an unsteady stretching sheet*, International Journal of Thermal Sciences **47**, No. 6 (2008) 766-72.

[29] AM. Megahed, *Effect of slip velocity on Casson thin film flow and heat transfer due to unsteady stretching sheet in presence of variable heat flux and viscous dissipation*, Applied Mathematics and Mechanics **36**, No. 10 (2015) 1273-84.

[30] S. Muhammad, G. Ali, Z. Shah, S. Islam, SA. Hussain, *The Rotating Flow of Magneto Hydrodynamic Carbon Nanotubes over a Stretching Sheet with the Impact of Non-Linear Thermal Radiation and Heat Generation/Absorption*, Applied Sciences **8**, No. 4 (2018) 482.

[31] S. Mustafa and S. un Nisa, *A Comparison of Single Server and Multiple Server Queuing Models in Different Departments of Hospitals*, Punjab Univ. j. math. **47**, No. 1 (2015) 73-80.

[32] S. Nadeem and M. Awais, *Thin film flow of an unsteady shrinking sheet through porous medium with variable viscosity*, Physics Letters A. **372**, No. 30 (2008)4965-72.

[33] M. Patel and MG. Timol, *Numerical treatment of PowellEyring fluid flow using method of satisfaction of asymptotic boundary conditions (MSABC)*, Applied Numerical Mathematics **59**, No. 10 (2009) 2584-92.

[34] MM. Rashidi, AM. Siddiqui and M. Asadi, *Application of homotopy analysis method to the unsteady squeezing flow of a second-grade fluid between circular plates*, Mathematical Problems in Engineering 2010.

[35] N. Raza, *Unsteady Rotational Flow of a Second GradeFluid with Non-Integer Caputo Time Fractional Derivative*, Punjab Univ. j. math. **49**, No. 3 (2017) 15-25.

[36] N. Sadiq, M. Imran, R. Safdar, M. Tahir, M. Younas and M. Javaid, *Exact Solution for Some Rotational Motions of Fractional Oldroyd-B Fluids Between Circular Cylinders*, Punjab Univ. j. math. **50**, No. 4 (2018) 39-59.

[37] R. Safdar, M. Imran, M. Tahir, N. Sadiq and M. A. Imran, *MHD Flow of Burgers Fluid under the Effect of Pressure Gradient Through a Porous Material Pipe*, Punjab Univ. j. math. **50**, No. 4 (2018) 73-90.

[38] Z. Shah, T. Gul, AM. Khan, I. Ali, S. Islam, F. Husain, *Effects of hall current on steady three dimensional non-newtonian nanofluid in a rotating frame with brownian motion and thermophoresis effects*, J. Eng. Technol. **6**, No. 1 (2017) 280-96.

[39] Z. Shah, S. Islam, T. Gul, E. Bonyah, MA. Khan, *The electrical MHD and hall current impact on micropolar nanofluid flow between rotating parallel plates*, Results in Physics **9**, No. 1 (2018) 1201-14.

[40] S. B. Shah, H. Shaikh, M. A. Solagni and A. Baloch, *Computer Simulation of Fibre Suspension Flow through a Periodically Constricted Tube*, Punjab Univ. j. math. **46**, No. 2 (2014) 19-34.

[41] V. Sirohi, MG. Timol and NL. Kalathia, *Numerical treatment of PowellEyring fluid flow past a 90 degree wedge*, Reg. J. Energy Heat Mass Transfer **6**, No. 3 (1984) 219-28.

[42] M. Suleman and S. Riaz, *Unconditionally Stable Numerical Scheme to Study the Dynamics of Hepatitis B Disease*, Punjab Univ. j. math. **49**, No. 3 (2017) 99-118.

[43] F. Tahir, T. Gul, S. Islam, Z. Shah, A. Khan, W. Khan and L. Ali, *Flow of a Nano-Liquid Film of Maxwell Fluid with Thermal Radiation and Magneto Hydrodynamic Properties on an Unstable Stretching Sheet*, Journal of Nanofluids **06**, No. 6 (2017) 1021-30.

[44] R. Usha and R. Sridharan, *The axisymmetric motion of a liquid film on an unsteady stretching surface*, Journal of fluids engineering **117**, No. 1 (1995) 81-5.

[45] C. Wang and I. Pop, *Analysis of the flow of a power-law fluid film on an unsteady stretching surface by means of homotopy analysis method*, Journal of Non-Newtonian Fluid Mechanics **138**, No. 3 (2006) 161-72.

[46] A. A. Zafar, M. B. Riaz and M. A. Imran, *Unsteady Rotational Flow of Fractional Maxwell Fluid in a Cylinder Subject to Shear Stress on the Boundary*, Punjab Univ. j. math. **50**, No. 2 (2018) 21-32.